

The $B - L$ Supersymmetric Standard Model with Inverse Seesaw at the Large Hadron Collider

S. Khalil^{1,2} and S. Moretti³

¹ *Center for Fundamental Physics, Zewail City for Science and Technology, 6 October City, Cairo, Egypt.*

² *Department of Mathematics, Faculty of Science, Ain Shams University, Cairo, 11566, Egypt.*

³ *School of Physics & Astronomy, University of Southampton, Highfield, Southampton, UK.*

Abstract

We review the TeV scale $B - L$ extension of the Minimal Supersymmetric Standard Model (BLSSM) where an inverse seesaw mechanism of light neutrino mass generation is naturally implemented and concentrate on its hallmark manifestations at the Large Hadron Collider (LHC).

1 Introduction

The solid experimental evidence for neutrino oscillations, pointing towards non-vanishing neutrino masses, is one of the few firm hints for physics beyond the Standard Model (SM). Neutrinos are strictly massless in the SM due to two main reasons: *(i)* the absence of right-handed neutrinos; *(ii)* the SM has an exact global Baryon minus Lepton ($B - L$) number conservation. The minimal extension of the SM, based on the gauge group $SU(3)_C \times SU(2)_L \times U(1)_Y \times U(1)_{B-L}$, can account for light neutrino masses through either a Type-I seesaw or an Inverse seesaw (IS) mechanism [1, 2]¹. In the type-I seesaw mechanism right-handed neutrinos acquire Majorana masses at the $B - L$ symmetry breaking scale, which can be related to the Supersymmetry (SUSY) breaking scale, *i.e.*, $\mathcal{O}(1)$ TeV [4]. In contrast, in the IS case, these Majorana masses are not allowed by the $B - L$ gauge symmetry and another pair of SM gauge singlet fermions with tiny masses ($\mathcal{O}(1)$ keV) must be introduced. One of these two singlets fermions couples to right-handed neutrinos and is involved in generating the light neutrino masses. The other singlet (which is usually called an inert neutrino) is completely decoupled and interacts only through the $B - L$ gauge boson, therefore it may account for warm Dark Matter (DM) [5], see also Refs. [6, 7]. In both scenarios, this $B - L$ model induces several testable signals at the LHC

¹For old attempts at analysing a high scale $B - L$ extension of the SM, see Ref. [3].

involving the new predicted particles: a Z' (neutral gauge boson associated with the $U(1)_{B-L}$ group), an extra Higgs state (an additional singlet state introduced to break the gauge group $U(1)_{B-L}$ spontaneously) and three (Type-I) or six (IS) heavy neutrinos, ν_h (that are required to cancel the associated anomaly and are necessary for the consistency of the model). This is the setup for the non-SUSY sector of the $B-L$ scenario, which is well established in the literature (see Refs. [8, 9] for a review of its main phenomenological manifestation).

It is the purpose of this paper to review its Supersymmetric version, the BLSSM, particularly in the IS framework. The plan of the paper is as follows. In the next section we proceed to the construction of the BLSSM Lagrangian. In Sect. 3 we describe how dynamical Electro-Weak Symmetry Breaking (EWSB) occurs in the BLSSM whereas in Sect. 4 we introduce its particle spectrum. (In Sect. 5 we study in particular the Higgs masses.) Then, in Sect. 6, we describe the main manifestations of the BLSSM at the LHC. We conclude in Sect. 7.

2 Constructing the BLSSM

The particle content of this model includes the following superfields in addition to those of the Minimal Supersymmetric Standard Model (MSSM): (i) two SM singlet chiral Higgs superfields $\chi_{1,2}$, whose Vacuum Expectation Values (VEVs) of their scalar components spontaneously break the $U(1)_{B-L}$ and χ_2 is required to cancel the $U(1)_{B-L}$ anomaly; (ii) three sets of SM singlet chiral superfields, $N_i, S_{1_i}, S_{2_i} (i = 1, 2, 3)$, to implement the IS mechanism (also in order to cancel the $B-L$ anomaly). Table 1 provides the particle content of the SUSY version of the $B-L$ model with IS (henceforth BLSSM-IS for short) as well as the different charge assignments of each Superfield.

	\hat{Q}_i	\hat{U}_i^c	\hat{D}_i^c	$\hat{\ell}_i$	\hat{E}_i^c	\hat{N}_i^c	\hat{S}_1	\hat{S}_2	\hat{H}_1	\hat{H}_2	$\hat{\chi}_1$	$\hat{\chi}_2$
$SU(3)_c$	3	$\bar{3}$	$\bar{3}$	1	1	1	1	1	1	1	1	1
$SU(2)_L$	2	1	1	2	1	1	1	1	2	2	1	1
$U(1)_Y$	1/6	-2/3	1/3	-1/2	1	0	0	0	-1/2	1/2	0	0
$U(1)_{B-L}$	1/6	1/6	1/6	-1/2	1/2	1/2	1	-1	0	0	1/2	-1/2

Table 1: Particle content of the BLSSM-IS.

The Superpotential of the leptonic sector in this model is given by

$$W = Y_E L H_1 E^c + Y_\nu L H_2 N^c + Y_S N^c \chi_1 S_2 + \mu H_1 H_2 + \mu' \chi_1 \chi_2. \quad (1)$$

Note that a Z_2 discrete symmetry is imposed to prevent undesired interactions between the \hat{S}_1 Superfield and the other ones, which would complicate the neutrino sector more than required. By assuming a minimal Supergravity (mSugra) inspired universality of parameters at the scale of a Grand Unification Theory (GUT), we obtain that the SUSY soft breaking Lagrangian is given by

$$\begin{aligned}
-\mathcal{L}_{\text{soft}} = & m_0^2 [|\tilde{Q}|^2 + |\tilde{U}|^2 + |\tilde{D}|^2 + |\tilde{L}|^2 + |\tilde{E}|^2 + |\tilde{N}|^2 + |\tilde{S}_1|^2 + |\tilde{S}_2|^2 + |H_1|^2 + |H_2|^2 + |\chi_1|^2 \\
& + |\chi_2|^2] + [Y_U^A \tilde{Q} H_2 \tilde{U}^c + Y_D^A \tilde{Q} H_1 \tilde{D}^c + Y_E^A \tilde{L} H_1 \tilde{E}^c + Y_\nu^A \tilde{L} H_2 \tilde{N}^c + Y_S^A \tilde{N}^c \chi_1 \tilde{S}_2] \\
& + [B(\mu H_1 H_2 + \mu' \chi_1 \chi_2) + h.c.] + \frac{1}{2} M_{1/2} [\tilde{g}^a \tilde{g}^a + \tilde{W}^a \tilde{W}^a + \tilde{B} \tilde{B} + \tilde{Z}' \tilde{Z}' + h.c.].
\end{aligned}$$

Therefore, the corresponding Lagrangian of the leptonic sector is given by [2]

$$\begin{aligned}
\mathcal{L}_{B-L} = & -\frac{1}{4} F'_{\mu\nu} F'^{\mu\nu} + i \bar{\ell}_L D_\mu \gamma^\mu \ell_L + i \bar{e}_R D_\mu \gamma^\mu e_R \\
& + i \bar{\nu}_R D_\mu \gamma^\mu \nu_R + i \bar{S}_1 D_\mu \gamma^\mu S_1 + i \bar{S}_2 D_\mu \gamma^\mu S_2 \\
& + (D^\mu \phi)^\dagger D_\mu \phi + (D^\mu \chi)^\dagger D_\mu \chi - V(\phi, \chi) \\
& - (\lambda_e \bar{\ell}_L \phi e_R + \lambda_\nu \bar{\ell}_L \tilde{\phi} \nu_R + \lambda_S \bar{\nu}_R^c \chi S_2) + h.c.
\end{aligned} \tag{2}$$

After the $B-L$ and EW symmetry breakings, through non-vanishing VEVs of χ ($|\langle \eta \rangle| = v'/\sqrt{2}$) and ϕ ($|\langle h \rangle| = v/\sqrt{2}$), one finds that the neutrino Yukawa interactions lead to the following mass terms [2]:

$$\mathcal{L}_m^\nu = m_D \bar{\nu}_L \nu_R + M_N \bar{\nu}_R^c S_2 + h.c., \tag{3}$$

where $m_D = \frac{1}{\sqrt{2}} \lambda_\nu v$ and $M_N = \frac{1}{\sqrt{2}} \lambda_S v'$. Here v' is assumed to be of order TeV and $v = 246$ GeV. Moreover, one may generate very small Majorana masses for the $S_{1,2}$ fermions through possible non-renormalisable terms like $\bar{S}_1^c \eta^{\dagger 4} S_1 / M^3$ and $\bar{S}_2^c \eta^4 S_2 / M^3$. Hence, the Lagrangian of neutrino masses, in the flavour basis, is given by

$$\mathcal{L}_m^\nu = \mu_s \bar{S}_2^c S_2 + (m_D \bar{\nu}_L \nu_R + M_N \bar{\nu}_R^c S_2 + h.c.), \tag{4}$$

where $\mu_s = \frac{v^4}{4M^3} \lesssim 10^{-6}$ GeV. Therefore, the neutrino mass matrix can be written as $\mathcal{M}_\nu \bar{\psi}^c \psi$ with $\psi = (\nu_L^c, \nu_R, S_2)$ and \mathcal{M}_ν is given by

$$\mathcal{M}_\nu = \begin{pmatrix} 0 & m_D & 0 \\ m_D^T & 0 & M_N \\ 0 & M_N^T & \mu_s \end{pmatrix}. \tag{5}$$

Note that, in order to avoid a possible large mass term $m S_1 S_2$ in the Lagrangian, Eq.(2), that would spoil the above IS structure, one assumes that the SM particles, ν_R , χ , and S_2

are even under a Z_2 -symmetry, while S_1 is an odd particle. Also other discrete symmetries may be used to avoid other possible non-renormalisable terms [10].

The diagonalisation of the mass matrix, Eq.(5), leads to the following light and heavy neutrino masses, respectively:

$$m_{\nu_i} = m_D M_R^{-1} \mu_s (M_R^T)^{-1} m_D^T, \quad (6)$$

$$m_{\nu_H} = m_{\nu_{H'}} = \sqrt{M_R^2 + m_D^2}. \quad (7)$$

Thus, one finds that the light neutrino masses can be of order eV, with a TeV scale M_R , if $\mu_s \ll M_R$, and a order one Yukawa coupling λ_ν . Such large coupling is crucial for testing the BLSSM with IS (henceforth BLSSM-IS for short) and probing the heavy neutrinos at the LHC. From Eq. (6), one finds that the 9×9 neutrino mass matrix \mathcal{M}_ν can be diagonalised by the matrix V , *i.e.*, $V^T \mathcal{M}_\nu V = \mathcal{M}_\nu^{\text{diag}}$ [10], where

$$V = \begin{pmatrix} V_{3 \times 3} & V_{3 \times 6} \\ V_{6 \times 3} & V_{6 \times 6} \end{pmatrix}, \quad (8)$$

with $V_{3 \times 3}$ given by

$$V_{3 \times 3} \simeq \left(1 - \frac{1}{2} F F^T\right) U_{\text{MNS}}. \quad (9)$$

The matrix $V_{3 \times 6}$ is defined as

$$V_{3 \times 6} = (\mathbf{0}_{3 \times 3}, F) V_{6 \times 6}, \quad F = m_D M_R^{-1}. \quad (10)$$

Finally, $V_{6 \times 6}$ is the matrix that diagonalises the $\{\nu_R, S_2\}$ mass matrix. In order to guarantee that the first three eigenvalues of the light neutrino mass matrix \mathcal{M}_ν are consistent with the physical light neutrinos, one writes the Dirac neutrino mass matrix m_D as

$$m_D = U_{\text{MNS}} \sqrt{m_{\nu_i}^{\text{diag}}} R \sqrt{\mu_s^{-1}} M_N, \quad (11)$$

where R is an arbitrary orthogonal matrix.

As shown in [10], the mixings between light and heavy neutrinos are of order $\mathcal{O}(0.01)$. Therefore, the decay widths of these heavy neutrinos into SM fermions are sufficiently large. It is worth mentioning that the second SM singlet fermion, S_1 , remains light with mass given by

$$m_{S_1} = \mu_s \simeq \mathcal{O}(1) \text{ keV}, \quad (12)$$

where S_1 is a sort of inert neutrino that has no mixing with the active neutrinos. It can therefore be a good candidate for warm DM as emphasised in Ref. [5].

3 Radiative $B - L$ symmetry breaking in the BLSSM-IS

The stability condition for the scalar potential

$$V(\chi_1, \chi_2) = \mu_1^2 |\chi_1|^2 + \mu_2^2 |\chi_2|^2 - \mu_3^2 (\chi_1 \chi_2 + h.c.) + \frac{1}{2} g_{BL}^2 (|\chi_2|^2 - |\chi_1|^2)^2 \quad (13)$$

is given by

$$2\mu_3^2 < \mu_1^2 + \mu_2^2. \quad (14)$$

The minimisation of this potential, $\frac{\partial V}{\partial \chi_i} = 0$, $i = 1, 2$, implies that

$$\mu_1^2 = \mu_3^2 \cot \theta + \frac{M_{Z'}^2}{4} \cos 2\theta, \quad (15)$$

$$\mu_2^2 = \mu_3^2 \tan \theta - \frac{M_{Z'}^2}{4} \cos 2\theta. \quad (16)$$

From (15)–(16), one gets

$$\sin 2\theta = \frac{2\mu_3^2}{m_{A_0}^2}, \quad (17)$$

where $m_{A_0}^2 = \mu_1^2 + \mu_2^2$. Also note that, from (15)–(16), we get

$$v'^2 = \frac{(\mu_1^2 - \mu_2^2) - (\mu_1^2 + \mu_2^2) \cos 2\theta}{2g_{BL}^2 \cos 2\theta}. \quad (18)$$

Now we complete our analysis of symmetry breaking. We have

$$V_{11}(v'_1, v'_2) = 2\mu_1^2 - 2g_{BL}^2 (v_2'^2 - 3v_1'^2), \quad (19)$$

$$V_{12}(v'_1, v'_2) = -2\mu_3^2 - 4g_{BL}^2 v'_1 v'_2, \quad (20)$$

$$V_{22}(v'_1, v'_2) = 2\mu_2^2 + 2g_{BL}^2 (3v_2'^2 - v_1'^2), \quad (21)$$

where $V_{ij} = \frac{\partial^2 V(\chi_1, \chi_2)}{\partial \chi_i \partial \chi_j}$. To show that the symmetry will be broken spontaneously, we must ensure that the point $(v'_1, v'_2) = (0, 0)$ is not a local minimum of the potential V . Since $(V_{11}V_{22} - V_{12}^2)(0, 0) = (2\mu_1^2)(2\mu_2^2) - (2\mu_3^2)^2$ and $V_{11}(0, 0) = 2\mu_1^2 > 0$ we should impose a condition to make $(0, 0)$ a saddle point. This condition is

$$\mu_1^2 \mu_2^2 < \mu_3^4. \quad (22)$$

It is worth noting that it is impossible to simultaneously fulfill both the conditions (14) and (22) for positive values of μ_1^2 and μ_2^2 . To resolve this paradox, it must be clear that condition (14) is valid only at the GUT scale whereas condition (22) is valid at the $B - L$ symmetry breaking scale. However, in the running of the Renormalisation Group Equations (RGEs), from the GUT scale down to the $B - L$ breaking scale, one finds that

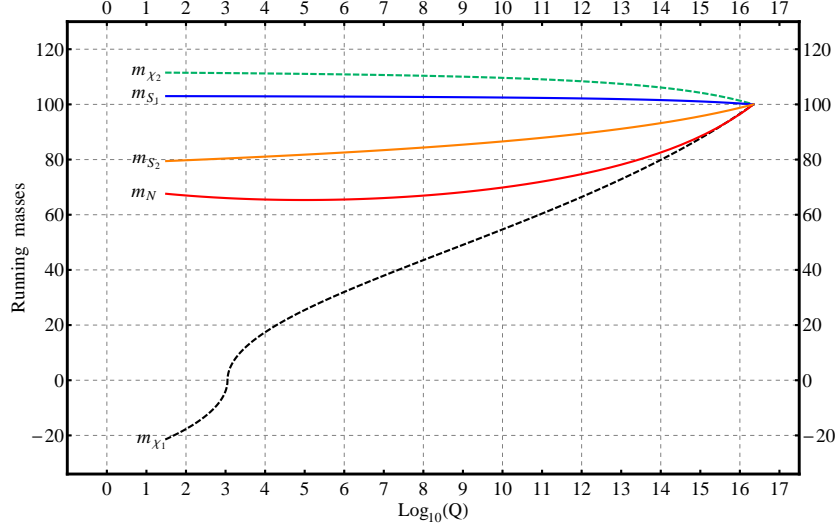


Figure 1: The evolution of the $B - L$ scalar masses from the GUT to the TeV scale for $m_0 = M_{1/2} = A_0 = 100$ GeV and $Y_{N_3} \sim \mathcal{O}(0.1)$.

the masses of the of Higgs singlets χ_1 and χ_2 run differently in such a way that $m_{\chi_1}^2$ can become negative whereas $m_{\chi_2}^2$ remains positive.

The RGEs for $\chi_{1,2}$ are given by

$$16\pi^2 \frac{dm_{\chi_1}^2}{dt} = -12g_{BL}^2 M_{BL}^2 + 6Y_{N_3}^2 (m_{\chi_1}^2 + m_{N_3}^2 + m_{S_{2_3}}^2 + A_{N_3}^2), \quad (23)$$

$$16\pi^2 \frac{dm_{\chi_2}^2}{dt} = -12g_{BL}^2 M_{BL}^2, \quad (24)$$

and in order to solve these we should take into account the following RGEs

$$16\pi^2 \frac{dg_3}{dt} = -3g_3^3, \quad (25)$$

$$16\pi^2 \frac{dg_2}{dt} = g_2^3, \quad (26)$$

$$16\pi^2 \frac{dg_1}{dt} = \frac{33}{5}g_1^3, \quad (27)$$

$$16\pi^2 \frac{dg_{BL}}{dt} = \frac{45}{5}g_{BL}^3, \quad (28)$$

$$16\pi^2 \frac{dM_1}{dt} = -6g_3^2 M_3, \quad (29)$$

$$16\pi^2 \frac{dM_1}{dt} = 2g_2^2 M_2, \quad (30)$$

$$16\pi^2 \frac{dM_1}{dt} = \frac{66}{2}g_1^2 M_1, \quad (31)$$

$$16\pi^2 \frac{dM_{BL}}{dt} = \frac{45}{2}g_{BL}^2 M_{BL}, \quad (32)$$

$$16\pi^2 \frac{dY_{N_3}}{dt} = Y_{N_3} \left(-\frac{9}{2}g_{BL}^2 + 5Y_{N_3}^2 + 2Y_{\nu_3}^2 \right), \quad (33)$$

$$16\pi^2 \frac{dY_{\nu_3}}{dt} = Y_{\nu_3} \left(-3g_2^2 - \frac{3}{5}g_1^2 - \frac{3}{2}g_{BL}^2 + Y_{N_3}^2 + 3Y_t^2 + 6Y_{\nu_3}^2 \right), \quad (34)$$

$$16\pi^2 \frac{dY_t}{dt} = Y_t \left(-\frac{16}{3}g_3^2 - 3g_2^2 - \frac{13}{15}g_1^2 - \frac{1}{6}g_{BL}^2 + 6Y_t^2 + 3Y_{\nu_3}^2 \right), \quad (35)$$

$$16\pi^2 \frac{dm_{N_3}^2}{dt} = -3g_{BL}^2 M_{BL}^2 + 2Y_N^2 \left(m_{\chi_1}^2 + m_{N_3}^2 + A_{N_3}^2 + m_{S_{23}}^2 \right) + 4Y_\nu^2 \left(m_{H_u}^2 + m_{N_3}^2 \right), \quad (36)$$

$$16\pi^2 \frac{dm_{S_{23}}^2}{dt} = -3g_{BL}^2 M_{BL}^2 + 2Y_N^2 \left(m_{\chi_1}^2 + m_{N_3}^2 + A_{N_3}^2 + m_{S_{23}}^2 \right), \quad (37)$$

$$16\pi^2 \frac{dA_{N_3}}{dt} = 10Y_{N_3}^2 A_{N_3} + 4A_{\nu_3} Y_{\nu_3}^2 + 9g_{BL}^2 M_{BL}, \quad (38)$$

$$16\pi^2 \frac{dA_{\nu_3}}{dt} = 12A_{\nu_3} Y_{\nu_3}^2 + 2Y_{N_3}^2 A_{N_3} + Y_t^2 A_t + 3g_2^2 M_2 + \frac{6}{5}g_1^2 M_1 + 3g_{BL}^2 M_{BL}, \quad (39)$$

$$16\pi^2 \frac{dA_t}{dt} = 12A_t Y_t^2 + 6Y_{\nu_3}^2 A_{\nu_3} + \frac{32}{3}g_3^2 M_3 + 6g_2^2 M_2 + \frac{26}{15}g_1^2 M_1 + \frac{1}{3}g_{BL}^2 M_{BL}, \quad (40)$$

$$16\pi^2 \frac{dm_{H_u}^2}{dt} = -6g_2^2 M_2^2 - \frac{6}{5}g_1^2 M_1^2 + 6Y_t^2 \left(A_t^2 + m_{Q_3}^2 + m_{U_3}^2 + m_{H_u}^2 \right) + 6Y_\nu^2 \left(A_{\nu_3}^2 + m_{N_3}^2 + m_{H_u}^2 \right), \quad (41)$$

$$16\pi^2 \frac{dm_{Q_3}^2}{dt} = -\frac{32}{3}g_3^2 M_3^2 - 6g_2^2 M_2^2 - \frac{2}{15}g_1^2 M_1^2 - \frac{1}{3}g_{BL}^2 M_{BL}^2 + 2Y_t^2 \left(A_t^2 + m_{Q_3}^2 + m_{U_3}^2 + m_{H_u}^2 \right), \quad (42)$$

$$16\pi^2 \frac{dm_{U_3}^2}{dt} = -\frac{32}{3}g_3^2 M_3^2 - \frac{32}{15}g_1^2 M_1^2 - \frac{1}{3}g_{BL}^2 M_{BL}^2 + 4Y_t^2 \left(A_t^2 + m_{Q_3}^2 + m_{U_3}^2 + m_{H_u}^2 \right). \quad (43)$$

Fig. 1 reports the result of the running. In plotting this figure, we set the following mSUGRA inspired conditions at the high scale, *e.g.*, $m_0 = M_{1/2} = A_0 = 100$ GeV and order one $Y_{N_3} \simeq M_{N_3}/v'$. As can be seen from the plot, $m_{\chi_1}^2$ drops rapidly to a negative mass region whereas $m_{\chi_2}^2$ remains positive. Also in Fig. 1, we plot the scale evolution for the scalar mass m_{N_3} as well as of $m_{S_{13}}$ and $m_{S_{23}}$. The figure illustrates that they remain positive at the TeV scale. Therefore, the $B - L$ breaking via a non-vanishing VEV for right-handed sneutrinos does not occur in the present framework.

4 The BLSSM-IS Spectrum

We have seen the evolution of different parameters from the GUT to the $B - L$ scale. Once the $B - L$ symmetry is broken and so is the EW one too (at the M_W scale), different particles with different quantum numbers can mix and acquire new mass eigenstates. Here, we will focus on the new particles associated with the $B - L$ symmetry, namely, the Z' gauge boson, extra Higgs bosons and right-handed sneutrinos. We shall do so in three separate subsections.

4.1 The Z' Gauge Boson in the BLSSM-IS

After the $B - L$ symmetry breaking, the new gauge boson, Z' , acquires its mass from the kinetic term of the $B - L$ Higgs fields, $\chi_{1,2}$. Namely, we have

$$M_{Z'}^2 = g_{BL}^2 v'^2 + \frac{1}{4} \tilde{g}^2 v^2, \quad (44)$$

where \tilde{g} is the gauge coupling mixing between $U(1)_Y$ and $U(1)_{B-L}$ and $v' = \sqrt{v_1'^2 + v_2'^2}$, wherein the VEVs of the $B - L$ Higgs fields are given by $\langle \text{Re} \chi_i^0 \rangle = \frac{v_i'}{\sqrt{2}}$. Furthermore, the mixing angle between the SM Z and the BLSSM Z' is given by

$$\tan 2\theta' = \frac{2\tilde{g}\sqrt{g_1^2 + g_2^2}}{\tilde{g}^2 + 16\left(\frac{v'}{v}\right)^2 g_{BL}^2 - g_2^2 - g_1^2}. \quad (45)$$

4.2 The Higgs Bosons in the BLSSM-IS

The gauge kinetic term induces mixing at tree level between the $H_{1,2}^0$ and $\chi_{1,2}^0$ states in the BLSSM scalar potential. Therefore, the minimisation conditions of this potential at tree level lead to the following relations [11]:

$$B_\mu = -\frac{1}{8} \left[-2\tilde{g}g_{BL}v'^2 \cos 2\beta' + 4m_{H_1}^2 - 4m_{H_2}^2 + (g_1^2 + \tilde{g}^2 + g_2^2)v^2 \cos 2\beta \right] \tan 2\beta, \quad (46)$$

$$B_{\mu'} = \frac{1}{4} \left[-2g_{BL}^2 v'^2 \cos 2\beta' + 2m_{\chi_1}^2 - 2m_{\chi_2}^2 + \tilde{g}g_{BL}v^2 \cos 2\beta \right] \tan 2\beta', \quad (47)$$

where $\tan \beta = \frac{v_2}{v_1}$ and $\tan \beta' = \frac{v_1'}{v_2'}$. Note that, with non-vanishing \tilde{g} , the B_μ parameter depends on v' and the sign of $\cos 2\beta'$. We may have both constructive and destructive interference between the first term and other terms in Eq. (46). In general, we find that the typical value of B_μ is of order TeV.

To obtain the masses of the physical neutral Higgs bosons, one makes the usual redefinition of the Higgs fields, i.e., $H_{1,2}^0 = \frac{1}{\sqrt{2}}(v_{1,2} + \sigma_{1,2} + i\phi_{1,2})$ and $\chi_{1,2}^0 = \frac{1}{\sqrt{2}}(v'_{1,2} + \sigma'_{1,2} + i\phi'_{1,2})$, where $\sigma_{1,2} = \text{Re}H_{1,2}^0$, $\phi_{1,2} = \text{Im}H_{1,2}^0$, $\sigma'_{1,2} = \text{Re}\chi_{1,2}^0$ and $\phi'_{1,2} = \text{Im}\chi_{1,2}^0$. The real parts correspond to the CP-even Higgs bosons and the imaginary parts correspond to the CP-odd Higgs bosons. The squared-mass matrix of the BLSSM CP-odd neutral Higgs fields at tree level, in the basis $(\phi_1, \phi_2, \phi'_1, \phi'_2)$, is given by

$$m_{A,A'}^2 = \begin{pmatrix} B_\mu \tan \beta & B_\mu & 0 & 0 \\ B_\mu & B_\mu \cot \beta & 0 & 0 \\ 0 & 0 & B_{\mu'} \tan \beta' & B_{\mu'} \\ 0 & 0 & B_{\mu'} & B_{\mu'} \cot \beta' \end{pmatrix}. \quad (48)$$

It is clear that the MSSM-like CP-odd Higgs A is decoupled from the BLSSM-like one A' (at tree level). However, due to the dependence of B_μ on v' , one may find $m_A^2 = \frac{2B_\mu}{\sin 2\beta} \sim m_{A'}^2 = \frac{2B_{\mu'}}{\sin 2\beta'} \sim \mathcal{O}(1 \text{ TeV})$.

The squared-mass matrix of the BLSSM CP-even neutral Higgs fields at tree level, in the basis $(\sigma_1, \sigma_2, \sigma'_1, \sigma'_2)$, is given by

$$M^2 = \begin{pmatrix} M_{hH}^2 & M_{hh'}^2 \\ M_{hh'}^{2T} & M_{h'H'}^2 \end{pmatrix}, \quad (49)$$

where M_{hH}^2 is the usual MSSM neutral CP-even Higgs mass matrix, which leads to the SM-like Higgs boson with mass, at one loop level, of order 125 GeV and a heavy Higgs boson with mass $m_H \sim m_A \sim \mathcal{O}(1 \text{ TeV})$. In this case, the BLSSM matrix $M_{h'H'}^2$ is given by

$$M_{h'H'}^2 = \begin{pmatrix} m_{A'}^2 c_{\beta'}^2 + g_{BL}^2 v_1'^2 & -\frac{1}{2} m_{A'}^2 s_{2\beta'} - g_{BL}^2 v_1' v_2' \\ -\frac{1}{2} m_{A'}^2 s_{2\beta'} - g_{BL}^2 v_1' v_2' & m_{A'}^2 s_{\beta'}^2 + g_{BL}^2 v_2'^2 \end{pmatrix}, \quad (50)$$

where $c_x = \cos(x)$ and $s_x = \sin(x)$. Therefore, the eigenvalues of this mass matrix are given by

$$m_{h',H'}^2 = \frac{1}{2} \left[(m_{A'}^2 + M_{Z'}^2) \mp \sqrt{(m_{A'}^2 + M_{Z'}^2)^2 - 4m_{A'}^2 M_{Z'}^2 \cos^2 2\beta'} \right]. \quad (51)$$

If $\cos^2 2\beta' \ll 1$, one finds that the lightest $B - L$ neutral Higgs state is given by

$$m_{h'} \simeq \left(\frac{m_{A'}^2 M_{Z'}^2 \cos^2 2\beta'}{m_{A'}^2 + M_{Z'}^2} \right)^{\frac{1}{2}} \simeq \mathcal{O}(100 \text{ GeV}). \quad (52)$$

The mixing matrix $M_{hh'}^2$ is proportional to \tilde{g} and can be written as [11]

$$M_{hh'}^2 = \frac{1}{2} \tilde{g} g_{BL} \begin{pmatrix} v_1 v_1' & -v_1 v_2' \\ -v_2 v_1' & v_2 v_2' \end{pmatrix}. \quad (53)$$

For a gauge coupling $g_{BL} \sim |\tilde{g}| \sim \mathcal{O}(0.5)$, these off-diagonal terms are about one order of magnitude smaller than the diagonal ones. However, they are still crucial for generating interaction vertices between the genuine BLSSM Higgs bosons and the MSSM-like Higgs states. Note that the mixing gauge coupling constant, \tilde{g} , is a free parameter that can be positive or negative [11].

In Fig. 2, we show the masses of the four CP-even Higgs bosons in the BLSSM for $g_{BL} = 0.4$ and $\tilde{g} = -0.4$. In this plot we fix the lightest MSSM Higgs boson mass to

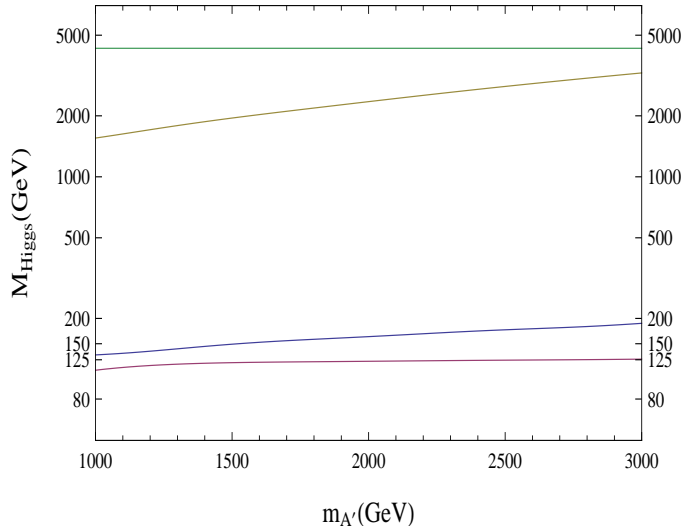


Figure 2: The BLSSM CP-even Higgs masses versus $m_{A'}$ for $g_{BL} = 0.4$ and $\tilde{g} = -0.4$.

be of order 125 GeV. As can be seen from this figure, as intimated, one of the BLSSM Higgs bosons, h' , can be the second lightest Higgs boson (~ 137 GeV). Both H and H' are instead quite heavy (since both m_A and $m_{A'}$ are of order TeV).

This sets the stage for the hypothesis made in Ref. [12] (see also [13]), wherein, motivated by a $\sim 2.9\sigma$ excess recorded by the CMS experiment at the LHC around a mass of order ~ 137 GeV in $ZZ \rightarrow 4l$ and $\gamma\gamma$ samples, it was shown that a double Higgs peak structure can be generated in the BLSSM, with CP-even Higgs boson masses at ~ 125 and ~ 137 GeV, a possibility instead precluded to the MSSM.

Before proceeding in this respect, though, two remarks are in order: firstly, if $\tilde{g} = 0$, the coupling of the BLSSM lightest Higgs state, h' , with the SM particles will be significantly suppressed ($\leq 10^{-5}$ relative to the SM strength), so that, in order to account for possible h' signals at the LHC, this parameter ought to be sizable; secondly, in both cases of vanishing and non-vanishing \tilde{g} , one may fine-tune the parameters and get a light m_A , which leads to a MSSM-like CP-even Higgs state, H , with $m_H \sim 137$ GeV. However, it is well known that in the MSSM the coupling HZZ is suppressed with respect to the corresponding one of the SM-like Higgs particle by one order of magnitude due to the smallness of $\cos(\beta - \alpha)$, where $\sin(\beta - \alpha) \sim 1$. In addition, the total decay width of H is larger than the total decay width of the SM-like Higgs, h , by at least one order of magnitude, because it is proportional to $(\cos \alpha / \cos \beta)^2$, which is essentially the square of the coupling of H to the bottom quark. Therefore, the MSSM-like heavy Higgs signal ($pp \rightarrow H \rightarrow ZZ \rightarrow 4l$) has a very suppressed cross section and thus cannot be a candidate for light Higgs signals at the LHC.

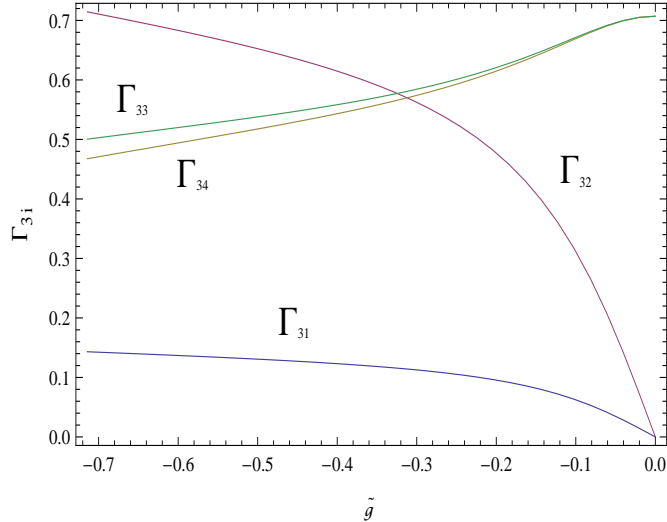


Figure 3: The mixing of h' , Γ_{3i} , versus the gauge kinetic mixing, \tilde{g} .

In the light of this, we will focus in the next section on the lightest BLSSM CP-even Higgs, h' , as a possible candidate for the second Higgs peak seen by CMS in Ref. [14]. However, before doing so, we ought to setup appropriately the BLSSM parameter space, in order to find such a solution. As mentioned above, the recent results from CMS indicate a $\sim 2.9\sigma$ hint of a second Higgs boson at 137 GeV or above. Herein, for definiteness, we consider $m_{h'} = 136.5$ GeV as reference BLSSM point.

As emphasised above, in the BLSSM, it is quite natural to have two light CP-even Higgs bosons, h and h' , with mass 125 GeV and ~ 137 GeV, respectively. The CP-even neutral Higgs mass matrix in Eq. (49) can be diagonalised by a unitary transformation:

$$\Gamma M^2 \Gamma^\dagger = \text{diag}\{m_h^2, m_H^2, m_{h'}^2, m_{H'}^2\}. \quad (54)$$

The mixing couplings Γ_{32} and Γ_{31} are proportional to \tilde{g} and they identically vanish if $\tilde{g} = 0$, as one can see in Fig. 3. Also, in this limit, Γ_{11} and Γ_{12} approach $\sin \alpha$ and $\cos \alpha$, respectively, where α is the usual CP-even Higgs mixing angle in the MSSM.

The lightest eigenstate h is the SM-like Higgs boson, for which we will fix its mass to be exactly 125 GeV. As mentioned, numerical scans of the BLSSM parameter space confirm that the h' state can then be the second light Higgs boson with mass of $\mathcal{O}(137)$ GeV). The other two CP-even states, H and H' , are heavy (of $\mathcal{O}(1)$ TeV). The h' can be written in terms of gauge eigenstates as

$$h' = \Gamma_{31} \sigma_1 + \Gamma_{32} \sigma_2 + \Gamma_{33} \sigma'_1 + \Gamma_{34} \sigma'_2. \quad (55)$$

Thus, the couplings of the h' with up- and down-quarks are given by

$$h' u \bar{u} : -i \frac{m_u}{v} \frac{\Gamma_{32}}{\sin \beta}, \quad h' d \bar{d} : -i \frac{m_d}{v} \frac{\Gamma_{31}}{\cos \beta}. \quad (56)$$

Similarly, one can derive the h' couplings with the W^+W^- and ZZ gauge boson pairs:

$$\begin{aligned} h' W^+ W^- & : i g_2 M_W (\Gamma_{32} \sin \beta + \Gamma_{31} \cos \beta), \\ h' ZZ & : \frac{i}{2} \left[4g_{BL} \sin^2 \theta' (v'_1 \Gamma_{32} + v'_2 \Gamma_{31}) \right. \\ & \quad \left. + (v_2 \Gamma_{32} + v_1 \Gamma_{31}) (g_z \cos \theta' - \tilde{g} \sin \theta')^2 \right]. \end{aligned}$$

Since $\sin \theta' \ll 1$, the coupling of the h' with ZZ , $g_{h'ZZ}$, will be as follows:

$$g_{h'ZZ} \simeq i g_z M_Z (\Gamma_{32} \sin \beta + \Gamma_{31} \cos \beta), \quad (57)$$

where $g_z = \sqrt{g_1^2 + g_2^2}$. In the analysis below we have used the SARAH [15] and SPheno [16, 17] to build the BLSSM. Furthermore, the matrix-element calculation and event generation were derived from MadGraph 5 [18] and manipulated with MadAnalysis 5 [19]. Finally, notice that all current experimental constraints, from both collider (LEP2, Tevatron and LHC) and flavour (BaBar, Belle and LHCb) are taken into account in our numerical scans.

In what follows, we will consider the BLSSM benchmark point for soft SUSY breaking parameters given in Table 2.

Inputs					
g_{BL}	\tilde{g}	$\tan \beta$	$\tan \beta'$	$M_{Z'}$	$m_{H_1}^2$
0.55	-0.12	5	1.15	1700	1.1×10^6
$m_{H_2}^2$	$m_{\chi_1}^2$	$m_{\chi_2}^2$	$Y_\nu^{\text{diag.}}$	$Y_N^{\text{diag.}}$	$\text{rmsign}(\mu, \mu')$
-1×10^7	-2.8×10^4	7.8×10^5	10^{-4}	0.43	1
$(m_q^2)^{\text{diag.}}$	$(m_\ell^2)^{\text{diag.}}$	$(m_d^2)^{\text{diag.}}$	$(m_u^2)^{\text{diag.}}$	$(m_e^2)^{\text{diag.}}$	$(m_\nu^2)^{\text{diag.}}$
3.9×10^7	3.1×10^5	4×10^7	4×10^7	1.8×10^5	7.9×10^5
Outputs					
m_h	$m_{h'}$	m_H	$m_{H'}$	m_A	$m_{A'}$
125	136.5	3.1×10^3	2.3×10^3	3.1×10^3	1.6×10^3

Table 2: BLSSM benchmark point in terms of inputs (to SARAH and SPheno) and outputs (used in our analysis). (Dimensions of masses (squared) are GeV (GeV²).)

4.3 Sneutrino Masses in the BLSSM-IS

Now we turn to the sneutrino squared-mass matrix. The complete scalar potential is given by

$$V_{\text{scalar}} = V_F + V_D + V_{\text{soft}}, \quad (58)$$

where the V_F of sneutrinos is given by

$$\begin{aligned} V_F|_{\tilde{\nu}} &= (m_D^2 + M^2)\tilde{\nu}_R^*\tilde{\nu}_R + m_D^2\tilde{\nu}_L^*\tilde{\nu}_L + m_D M\tilde{\nu}_L^*\tilde{S}_2 + m_D M\tilde{S}_2^*\tilde{\nu}_L + M^2\tilde{S}_2^*\tilde{S}_2 + \mu m_D \cot \beta \tilde{\nu}_L^*\tilde{\nu}_R^* \\ &+ \mu m_D \cot \beta \tilde{\nu}_L\tilde{\nu}_R + \mu' M \cot \theta \tilde{\nu}_R^*\tilde{S}_2^* + \mu' M \cot \theta \tilde{\nu}_R\tilde{S}_2 \end{aligned} \quad (59)$$

One can easily show that the following sneutrino contribution can be obtained from the D -terms:

$$V_D|_{\tilde{\nu}} = \frac{M_Z^2}{2} \cos 2\beta \tilde{\nu}_L^*\tilde{\nu}_L + M_{Z'}^2 \cos 2\theta (\tilde{\nu}_L^*\tilde{\nu}_L - \tilde{\nu}_R^*\tilde{\nu}_R + 2\tilde{S}_2^*\tilde{S}_2). \quad (60)$$

Finally, the sneutrino soft terms are given by

$$V_{\text{soft}}|_{\tilde{\nu}} = \tilde{\nu}_R^* + m_{\tilde{S}}^2\tilde{S}_2^*\tilde{S}_2 + m_D A_\nu \tilde{\nu}_L\tilde{\nu}_R + M A_S \tilde{\nu}_R^*\tilde{S}_2^* + M A_S \tilde{\nu}_R\tilde{S}_2. \quad (61)$$

Hence, in the basis $(\tilde{\nu}_L, \tilde{\nu}_L^*, \tilde{\nu}_R, \tilde{\nu}_R^*, \tilde{S}_2, \tilde{S}_2^*)$, we have

$$M_{\tilde{\nu}_{\text{soft}}}^2 = \begin{pmatrix} & \tilde{\nu}_L & \tilde{\nu}_L^* & \tilde{\nu}_R & \tilde{\nu}_R^* & \tilde{S}_2 & \tilde{S}_2^* \\ \tilde{\nu}_L^* & m_{LL}^2 & 0 & 0 & X_\nu & m_D M & 0 \\ \tilde{\nu}_L & 0 & m_{LL}^2 & X_\nu & 0 & 0 & m_D M \\ \tilde{\nu}_R^* & 0 & X_\nu & m_{RR}^2 & 0 & 0 & X_S \\ \tilde{\nu}_R & X_\nu & 0 & 0 & m_{RR}^2 & X_S & 0 \\ \tilde{S}_2^* & m_D M & 0 & 0 & X_S & m_{SS}^2 & 0 \\ \tilde{S}_2 & 0 & m_D M & X_S & 0 & 0 & m_{SS}^2 \end{pmatrix}, \quad (62)$$

where m_{LL}^2 , m_{RR}^2 and m_{SS}^2 are given by

$$m_{LL}^2 = m_{\tilde{L}}^2 + m_D^2 + 1/2(M_Z^2 \cos 2\beta + M_{Z'}^2 \cos 2\theta), \quad (63)$$

$$m_{RR}^2 = m_{\tilde{N}}^2 + m_D^2 + M^2 - \frac{M_{Z'}^2 \cos 2\theta}{2}, \quad (64)$$

$$m_{SS}^2 = m_{\tilde{S}}^2 + M^2 + M_{Z'}^2 \cos 2\theta. \quad (65)$$

Also X_ν and X_S are given by

$$X_\nu = m_D(A_\nu + \mu \cot \beta), \quad (66)$$

$$X_S = M(A_S + \mu' \cot \theta). \quad (67)$$

By defining CP-eigenstates as

$$\psi_L^+ = \frac{1}{\sqrt{2}}(\psi_L + \psi_L^*), \quad (68)$$

$$\psi_L^- = \frac{-i}{\sqrt{2}}(\psi_L - \psi_L^*), \quad (69)$$

one can write the sneutrino mass matrix $M_{\tilde{\nu}_{\text{soft}}}^2$ as

$$M_{\tilde{\nu}}^2 = \begin{pmatrix} \mathcal{M}_+^2 & 0 \\ 0 & \mathcal{M}_-^2 \end{pmatrix}, \quad (70)$$

where

$$\mathcal{M}_{\pm}^2 = \begin{pmatrix} m_L^2 + m_D^2 + \frac{M_Z^2 \cos 2\beta + M_{Z'}^2 \cos 2\theta}{2} & \pm m_D(A_\nu + \mu \cot \beta) & m_D M \\ \pm m_D(A_\nu + \mu \cot \beta) & m_N^2 + m_D^2 + M^2 - \frac{M_{Z'}^2}{2} \cos 2\theta & \pm M(A_S + \mu' \cot \theta) \\ m_D M & \pm M(A_S + \mu' \cot \theta) & m_S^2 + M^2 + M_{Z'}^2 \cos 2\theta \end{pmatrix}. \quad (71)$$

In fact, the diagonalisation process of such matrices, \mathcal{M}_{\pm}^2 , is not an easy task. Moreover, if we attempted to extract the eigenvalues of that matrix, we would obtain lengthy expressions from which it would be hard to gain any physics insight. Accordingly, we will approximate, carefully², the squared-mass matrix in Eq. (71) by adjusting the mixing parameters β and θ in order to remove the elements $(\mathcal{M}_{\pm}^2)_{12}$ and $(\mathcal{M}_{\pm}^2)_{23}$. It is clear that in this approximation \mathcal{M}_+^2 and \mathcal{M}_-^2 are identical and thus have identical eigenvalues³. That is, we can, from now on, call them $\mathcal{M}_{\tilde{\nu}}^2$ for short and double their eigenvalues. Explicitly, $\mathcal{M}_{\tilde{\nu}}^2$ is given by

$$\mathcal{M}_{\tilde{\nu}}^2 = \begin{pmatrix} m_L^2 + m_D^2 + \frac{M_Z^2 \cos 2\beta + M_{Z'}^2 \cos 2\theta}{2} & 0 & m_D M \\ 0 & m_N^2 + m_D^2 + M^2 - \frac{M_{Z'}^2}{2} \cos 2\theta & 0 \\ m_D M & 0 & m_S^2 + M^2 + M_{Z'}^2 \cos 2\theta \end{pmatrix}. \quad (72)$$

The eigenvalues of this matrix are given by

$$m_1^2 = d, \quad (73)$$

$$m_2^2 = \frac{1}{2} \left[(a + f) + \sqrt{(a - f)^2 + 4c^2} \right], \quad (74)$$

$$m_3^2 = \frac{1}{2} \left[(a + f) - \sqrt{(a - f)^2 + 4c^2} \right], \quad (75)$$

² By this we mean that the eigenvalues of the approximate squared-mass matrix must satisfy the limit of exact SUSY, as it will be clear from Eqs. (80)–(81).

³In fact, it can be proved that, in general, \mathcal{M}_+^2 and \mathcal{M}_-^2 have identical eigenvalues: this can easily be seen from the general procedure of calculating the eigenvalues of a matrix.

where

$$a = m_L^2 + m_D^2 + \frac{1}{2}(M_Z^2 \cos 2\beta + M_{Z'}^2 \cos 2\theta), \quad (76)$$

$$c = m_D M_N, \quad (77)$$

$$d = m_{\bar{N}}^2 + m_D^2 + M_N^2 - \frac{1}{2}M_{Z'}^2 \cos 2\theta, \quad (78)$$

$$f = m_{\bar{S}}^2 + M_N^2 + M_{Z'}^2 \cos 2\theta. \quad (79)$$

If one assumes that $m_{\bar{L}} = m_{\bar{N}} = m_{\bar{S}} = \tilde{m}$ and neglects the D -term, then the full set of sneutrino masses is given by

$$m_{\tilde{\nu}_{\ell_{1,2}}}^2 = \tilde{m}^2, \quad (80)$$

$$m_{\tilde{\nu}_{H_{3,4,5,6}}}^2 = m_D^2 + M_N^2 + \tilde{m}^2. \quad (81)$$

The phenomenological implications of right-handed neutrinos in type I seesaw BLSSM have been studied in Ref. [20]

5 (S)Neutrino Corrections to the Lightest Higgs Boson Mass

In this section, we calculate the one-loop radiative corrections due to right-handed (s)neutrinos to the mass of the lightest Higgs boson when the latter is SM-like. We show that such effects can be as large as $\mathcal{O}(100)$ GeV, thereby giving an absolute upper limit on such a mass around 170 GeV [21]. The importance of this result from a phenomenological point of view resides in the fact that this enhancement greatly reconciles theory and experiment, by alleviating the so-called ‘little hierarchy problem’ of the minimal SUSY realisation, whereby the currently measured mass of the SM-like Higgs mass is very near its absolute upper limit predicted theoretically, of 130 GeV.

It is important to note that, unlike the squark sector, where only the third generation (stops) has a large Yukawa coupling with the Higgs boson, hence giving the relevant correction to the Higgs mass, all three generations of the (s)neutrino sector may lead to important effects since the neutrino Yukawa couplings are generally not hierarchical. Also, due to the large mixing between the right-handed neutrinos N_i and S_{2_j} [22], all the right-handed sneutrinos $\tilde{\nu}_H$ are coupled to the Higgs boson H_2 , hence they can give significant contribution to the Higgs mass correction. In this respect, it is useful to note that the stop effect is due to the running of 12 degrees of freedom (3 colors times 2 charges times 2 for left and right stops) in the Higgs mass loop corrections, just like in the case of right-handed sneutrinos for which there are also 12 degrees of freedom (3 generations times 4 eigenvalues).

To calculate the (s)neutrino correction to the lightest Higgs mass, we computed, in the last section, the explicit form of the sneutrino masses, while for the neutrino mass expressions, which are well known, we refer the reader to [21]. Due to one generation of neutrinos and sneutrinos, the one-loop radiative correction to the effective potential is given by the relation

$$\Delta V_{\nu,\tilde{\nu}} = \frac{1}{64\pi^2} \left[\sum_{i=1}^6 m_{\tilde{\nu}_i}^4 \left(\log \frac{m_{\tilde{\nu}_i}^2}{Q^2} - \frac{3}{2} \right) - 2 \sum_{i=1}^3 m_{\nu_i}^4 \left(\log \frac{m_{\nu_i}^2}{Q^2} - \frac{3}{2} \right) \right]. \quad (82)$$

The first sum runs over the sneutrino mass eigenvalues, while the second sum runs over the neutrino masses (with vanishing m_{ν_1}). In case of degenerate diagonal Yukawa couplings, one finds that the total $\Delta V_{\nu,\tilde{\nu}}$ is given by three times the value of $\Delta V_{\nu,\tilde{\nu}}$ for one generation. This factor then compensates the colour factor of (s)top contributions.

Therefore, the genuine $B - L$ correction to the CP-even Higgs mass matrix, due to the (s)neutrinos, at the scale \hat{Q} at which $\frac{\partial(\Delta V_{\nu,\tilde{\nu}})}{\partial v_k} = 0$, is given by

$$\Delta M_{ij}^2 = \frac{1}{2} \frac{\partial^2(\Delta V_{\nu,\tilde{\nu}})}{\partial v_i \partial v_j}. \quad (83)$$

It follows that (see [21] for details)

$$\frac{\partial m_{\nu_\ell}^2}{\partial v_k} \simeq 0, \quad (84)$$

$$\frac{\partial m_{\nu_{H,H'}}^2}{\partial v_k} = 2Y_\nu v_k \delta_{k,2}. \quad (85)$$

Also from Eqs. (80)–(81), we have

$$\frac{\partial m_{\tilde{\nu}_{\ell 1,2}}^2}{\partial v_k} = 0, \quad (86)$$

$$\frac{\partial m_{\tilde{\nu}_{H3,4,5,6}}^2}{\partial v_k} = 2Y_\nu v_k \delta_{k,2}. \quad (87)$$

From the previous four equations, one can deduce that

$$\begin{aligned} \frac{\partial^2(\Delta V_{\nu,\tilde{\nu}})}{\partial v_k \partial v_\ell} &= \frac{1}{32\pi^2} \sum_i (-1)^{2J_i} (2J_i + 1) \frac{\partial m_i^2}{\partial v_k} \frac{\partial m_i^2}{\partial v_\ell} \log \frac{m_i^2}{Q^2} \\ &= \frac{1}{32\pi^2} \left[4(2Y_\nu^2 v_2)(2Y_\nu^2 v_2) \delta_{k,2} \delta_{\ell,2} \log \frac{m_{\tilde{\nu}_H}^2}{Q_0^2} - 2 \left(2(2Y_\nu^2 v_2)(2Y_\nu^2 v_2) \delta_{k,2} \delta_{\ell,2} \log \frac{m_{\nu_H}^2}{Q_0^2} \right) \right] \\ &= \frac{m_D^4}{2\pi^2 v_2^2} \log \left(\frac{m_{\tilde{\nu}_H}^2}{m_{\nu_H}^2} \right) \delta_{k,2} \delta_{\ell,2}. \end{aligned} \quad (88)$$

That is, we have

$$\Delta M_{11}^2 = \Delta M_{12}^2 = \Delta M_{21}^2 = 0, \quad (89)$$

$$\Delta M_{22}^2 = \frac{m_D^4}{4\pi^2 v_2^2} \log \frac{m_{\tilde{\nu}_H}^2}{m_{\nu_H}^2}. \quad (90)$$

Therefore, the complete one-loop squared-mass matrix of CP-even Higgs bosons will be given by $M_{\text{tree}}^2 + \Delta M^2$, with

$$\Delta M^2 = \begin{pmatrix} 0 & 0 \\ 0 & \delta_t^2 + \delta_\nu^2 \end{pmatrix}, \quad (91)$$

where δ_t^2 refers to the (s)top contribution presented in Eq. (1) of [21] and δ_ν^2 is the (s)neutrino correction given in Eq. (90). In this case, the lightest Higgs bosons mass is given by

$$m_h^2 = \frac{M_A^2 + M_Z^2 + \delta_t^2 + \delta_\nu^2}{2} \left[1 - \sqrt{1 - 4 \frac{M_Z^2 M_A^2 \cos^2 2\beta + (\delta_t^2 + \delta_\nu^2)(M_A^2 \sin^2 \beta + M_Z^2 \cos^2 \beta)}{(M_A^2 + M_Z^2 + \delta_t^2 + \delta_\nu^2)^2}} \right] \quad (92)$$

For $M_A \gg M_Z$ and $\cos 2\beta \simeq 1$, one finds that

$$m_h^2 \simeq M_Z^2 + \delta_t^2 + \delta_\nu^2. \quad (93)$$

If $\tilde{m} \simeq \mathcal{O}(1)$ TeV, $Y_\nu \simeq \mathcal{O}(1)$ and $M_N \simeq \mathcal{O}(500)$ GeV, one finds that $\delta_\nu^2 \simeq \mathcal{O}(100 \text{ GeV})^2$, thus the Higgs mass is of order $\sqrt{(90)^2 + \mathcal{O}(100)^2 + \mathcal{O}(100)^2} \text{ GeV} \simeq 170 \text{ GeV}$. It is worth mentioning that the choice of an order $\mathcal{O}(\infty)$ neutrino Yukawa coupling Y_ν at the $B - L$ scale must be tested. That is, we should ensure the absence of Landau poles during the run of the Yukawa coupling from the $B - L$ scale up to the GUT scale. This can be derived from the RGEs of the neutrino Yukawa coupling [15]:

$$16\pi^2 \frac{dY_\nu}{dt} = 3Y_\nu Y_\nu^\dagger Y_\nu + Y_\nu [\text{Tr}(Y_\nu Y_\nu^\dagger) + 3\text{Tr}(Y_u Y_u^\dagger) - \frac{3}{2}g_B^2 - \frac{3}{5}g_1^2 - 3g_2^2] + Y_\nu Y_S^* Y_S^T + Y_e^T Y_e^* Y_\nu, \quad (94)$$

$$16\pi^2 \frac{dY_u}{dt} = 3Y_u Y_u^\dagger Y_u + Y_u [\text{Tr}(Y_\nu Y_\nu^\dagger) + 3\text{Tr}(Y_u Y_u^\dagger) - \frac{1}{6}g_B^2 - \frac{13}{15}g_1^2 - 3g_2^2 - \frac{16}{3}g_3^2] + Y_u Y_d^\dagger Y_d, \quad (95)$$

$$16\pi^2 \frac{dY_S}{dt} = 2Y_S Y_S^\dagger Y_S + Y_S [\text{Tr}(Y_S Y_S^\dagger) - \frac{9}{2}g_B^2] + 2Y_\nu^T Y_\nu^* Y_S. \quad (96)$$

By ignoring the small Yukawa couplings, *i.e.*, Y_d and Y_e , one can solve these equations numerically and verify that, for $Y_t \simeq \mathcal{O}(1)$, the neutrino Yukawa coupling, Y_ν , at the TeV scale, can be of order one as well.

As an example of a generic 3×3 neutrino Yukawa coupling, Y_ν , we consider $Y_\nu = m_D/v_2$, with the Dirac neutrino mass matrix [10]

$$m_D = U_{\text{MNS}} \sqrt{m_{\nu\ell}^{\text{phys}}} R \sqrt{\mu_S^{-1}} M_N, \quad (97)$$

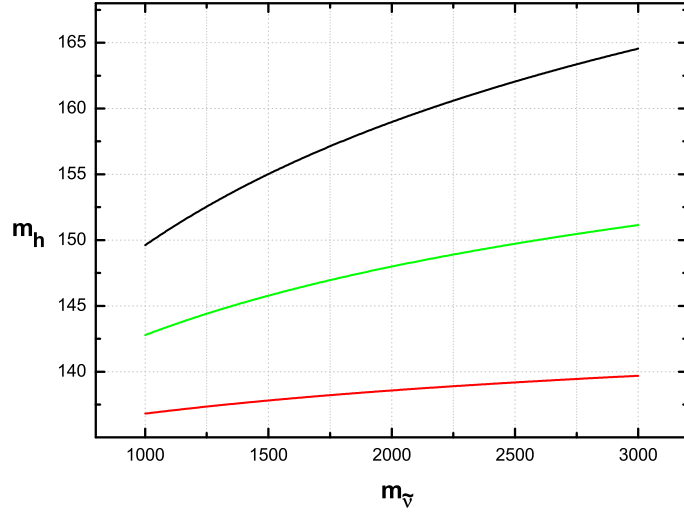


Figure 4: Lightest Higgs boson mass versus the lightest sneutrino mass for $M_N = \text{diag}\{300, 400, 500\}$, $Y_\nu = \text{diag}\{0, 0, 0.85\}$, $0.85 I_{3 \times 3}$, and U_{MNS} (for curves from bottom to top, respectively).

where R is an arbitrary orthogonal matrix and U_{MNS} is the light neutrino mixing matrix. If we assume that $R = I_{3 \times 3}$ and $\sqrt{m_{\nu\ell}^{\text{phys}}}/\mu_S \sim \mathcal{O}(0.1)$, then we find $Y_\nu \simeq U_{\text{MNS}}$. Note that here we assume a hierarchical μ_s in order to account for a possible hierarchy between light neutrino masses.

As shown in Fig. 5, these values of Y_ν are sufficient for enhancing the Higgs mass significantly. In this figure we present the Higgs mass, m_h , as a function of the sneutrino mass, $m_{\tilde{\nu}}$, for $M_N = \text{diag}\{300, 400, 500\}$ GeV and Y_ν couplings given by $Y_\nu = \text{diag}\{0, 0, 0.85\}$, $Y_\nu = 0.85 I_{3 \times 3}$, and $Y_\nu = U_{\text{MNS}}$. As can be seen, the neutrino Yukawa couplings indeed play a crucial role in enhancing the lightest Higgs mass, m_h . Also the large mixing in U_{MNS} is favoured by a large Higgs mass.

Finally, we consider the impact of the trilinear couplings A_N and A_S , which contribute to the off-diagonal elements of the sneutrino mass matrix (71). For simplicity, we assume $A_N = A_S = A_0$. In Fig. 5 we display the dependence of m_h on A_0 for the above mentioned three examples of Y_ν , $\tilde{m} = 2.5 I_{3 \times 3}$ TeV, and $M_N = \text{diag}\{300, 400, 500\}$ GeV. From this figure, it can be noted that a large value of A_0 may enhance the value of the Higgs mass by about 20 GeV. This can be understood as follows: for non-vanishing A_0 , one may approximate the sneutrino masses as

$$m_{\tilde{\nu}}^2 \simeq m_{\tilde{\nu}}^2|_{A_0=0} + \alpha m_D A_0, \quad (98)$$

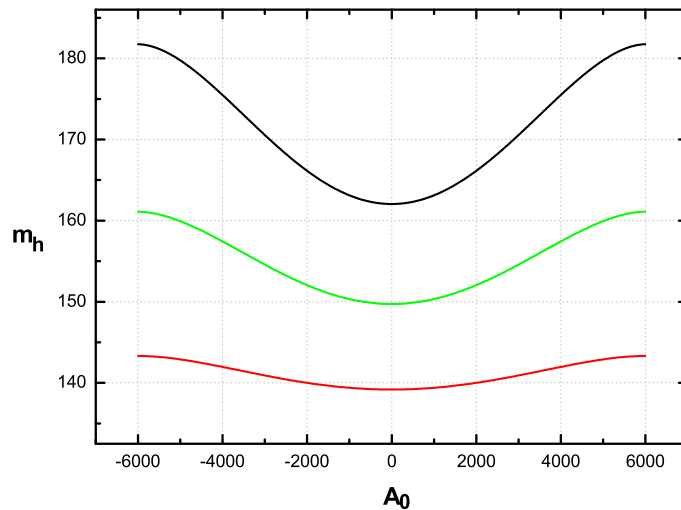


Figure 5: Lightest Higgs boson mass as a function of the trilinear coupling A_0 for $M_N = \text{diag}\{300, 400, 500\}$, $\tilde{m} = 2500 \text{ I}_{3 \times 3}$, $Y_\nu = \text{diag}\{0, 0, 0.85\}$, $0.85 \text{ I}_{3 \times 3}$ and U_{MNS} (for curves from bottom to top, respectively).

where the coefficient α can be fixed by fitting the sneutrino masses with this expression. Here we kept the dependence on the trilinear coupling to be consistent with the definition of the A -term leading to the expressions in the sneutrino squared-mass matrix (71), namely $A_{ij} = A_0 Y_{ij}$. In this case, Eq. (90) can be written as

$$\Delta M_{22} \simeq \frac{m_D^4}{4\pi^2 v_2^2} \left[\log \frac{m_{\tilde{\nu}_H}^2}{m_{\nu_H}^2} + \log \left(1 + \frac{\alpha m_D A_0}{m_{\nu_H}^2} \right) \right]. \quad (99)$$

Thus, for A_0 of order TeV, one finds that the Higgs mass is enhanced by few GeVs.

For such large A_ν -term, one should be careful with a possible $B-L$ symmetry breaking through a non-vanishing VEV of the sneutrino, which also breaks R -parity and makes the model quite involved. In order to avoid this minimum one has to satisfy the following constraint, which is very similar to the usual one imposed in the MSSM to avoid the electric-charge and color symmetry breaking minimum [23], namely

$$|A_\nu|^2 \leq 3 \left(m_L^2 + m_N^2 + m_{H_2}^2 \right). \quad (100)$$

Since we have m_L and m_N of order $|A_\nu|$, it is clear that this minimum can be safely avoided.

In relation to the measurements of the CMS and ATLAS experiments that indicate a mass for the discovered SM-like Higgs boson around 125 GeV, it is crucial to notice

that in the model described herein the required loop corrections to the Higgs mass can be obtained easily from a combination of the well established MSSM ones and those specific to the $B - L$ sector with stop and sneutrino masses that are smaller than 1 TeV, hence promptly testable at the LHC, while retaining a nature for the light Higgs state which is rather SM-like. Finally, it is also quite remarkable that our result remains valid for any model beyond the MSSM with TeV scale right-handed neutrinos (including Left-Right, Pati-Salam and other models derived from $SO(10)$).

6 LHC Signatures of the BLSSM-IS

6.1 Search for the BLSSM-IS Z'

Now we study the signatures of the extra neutral gauge boson Z' in the BLSSM-IS at the CERN machine⁴. The possibility of a Z' decay into a pair of heavy (inert) neutrinos would increase the total decay width of the Z' . Therefore, the Branching Ratio (BR) of $Z' \rightarrow l^+l^-$ ($l = e, \mu$), the prime Z' signal at the LHC, is suppressed with respect to the prediction of, *e.g.*, the Sequential Standard Model (SSM), which is usually considered as benchmark in experimental searches for a Z' . Fig. 6 shows the BRs of all Z' decays. According to this plot, the BRs of the non-SUSY Z' decays are given by [24]

$$\begin{aligned}
\sum_l BR(Z' \rightarrow l\bar{l} + \nu_l\bar{\nu}_l) &\sim 20.4\%, \\
\sum_q BR(Z' \rightarrow q\bar{q}) &\sim 9.2\%, \\
\sum_{\nu_h} BR(Z' \rightarrow \nu_h\bar{\nu}_h) &\sim 24\%, \\
\sum_{\nu_s} BR(Z' \rightarrow \nu_s\bar{\nu}_s) &\sim 41.4\%,
\end{aligned} \tag{101}$$

where, again, $l = e$ or μ , $q = u, d, s$, or c , ν_h refers to the six heavy neutrinos whereas ν_s refers to the three inert neutrinos. In this example we have assumed $M_{Z'} = 2$ TeV and heavy neutrino masses are set at 300, 500 and 630 GeV, respectively.

It is worth noting that, in our model, the Z' cross sections (σ 's) that were used to derive the ATLAS and CMS current mass limit could be simply rescaled by a factor of $(g_{B-L}/g_Z)^2 \times (1 - \text{BR}(Z' \rightarrow \text{new decay channels}))$. If $g_{B-L} = g_Z$ and $\text{BR}(Z' \rightarrow \text{new decay channels}) = 0$, this reproduces the SSM cross sections that were used by ATLAS and CMS. Considering the scaling of cross sections, the current Z' mass limits will

⁴In fact, we assume here that all SUSY particles (including sneutrinos) are large enough so that the Z' cannot decay into these, thereby implying that our analysis can be applied also to the standard $B - L$ scenario.

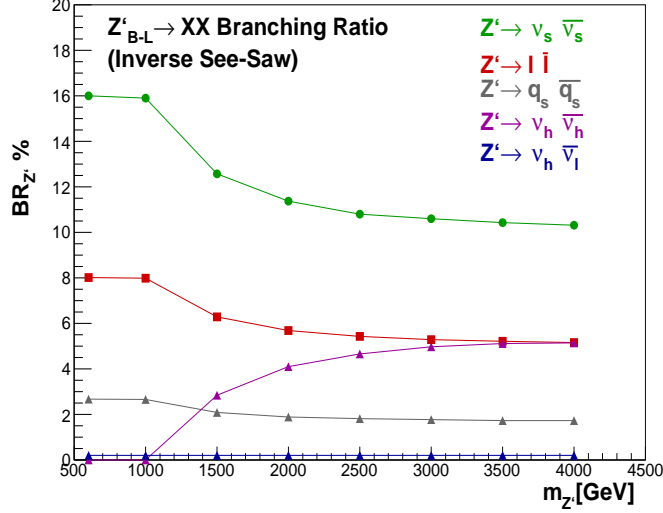


Figure 6: BRs of the Z' decays in the BLSSM-IS as a function of $M_{Z'}$. (Notice that fermion species are not summed over.)

Table 3: $Z' \rightarrow ee$ rates ($\sigma \times \text{BR}$) at different Z' masses.

$M_{Z'}$ [GeV]	σ_{SSM} [fb]	σ_{B-L} [fb] (with IS)		
		$g_{B-L} = g_Z$	$g_{B-L} = 0.5$	$g_{B-L} = 0.8$
1000	170	6	41	105.7
1500	21.7	0.58	4.5	13.2
2000	3.4	0.087	0.72	2.3
2500	0.8	0.015	0.15	0.58
3000	0.21	0.003	0.04	0.19

be lowered by a factor of $\sigma_{B-L}(Z' \rightarrow ll)/\sigma_{\text{SSM}}(Z' \rightarrow ll)$. This result is consistent with the conclusion of Ref. [25].

If $M'_{Z'} = 1000$ GeV were considered, $\text{BR}(Z' \rightarrow l^+l^-) \sim 14\%$ so that $\sigma \times \text{BR} = 16$ fb when $g_{B-L} = g_Z = 0.188$ and $\sigma \times \text{BR} = 82$ fb when $g_{B-L} = 0.5$, while in the SSM the $\text{BR}(Z' \rightarrow l^+l^-) \sim 7.6\%$ giving $\sigma \times \text{BR} = 340$ fb $^{-1}$ for both electron and muon channels. In this respect, the experimental limit $M_{Z'} \gtrsim 2.5$ TeV [26] (2.8 TeV [27]) will be lowered to 0.247 of its value when $g_{B-L} = 0.5$. Such a lower Z' mass is a striking signature of the BLSSM-IS. In the other scenario considered here, the Type-I BLSSM, the $\text{BR}(Z' \rightarrow l^+l^-) \sim 28.6\%$ and $\sigma \times \text{BR} = 814$ fb, that leads to increasing the current mass limit for $g_{B-L} = 0.5$. Table 3 gives $\sigma \times \text{BR}(Z' \rightarrow ee)$ for the SSM and BLSSM-IS at different g_{B-L} values.

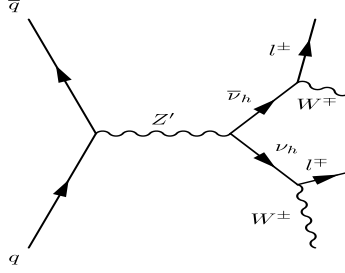


Figure 7: Feynman diagram for $q\bar{q} \rightarrow Z' \rightarrow \nu_h \bar{\nu}_h \rightarrow WWll$.

The dominant production mode for heavy neutrinos at the LHC would be through the Drell-Yan (DY) mechanism, mediated by the Z' . The mixing between light and heavy neutrinos generates new couplings between the heavy neutrinos, the weak gauge bosons Z, W and the associate leptons. These couplings are crucial for the decay of the heavy neutrinos. The main decay channel is through a W gauge boson, which may decay leptonically or hadronically. We sketch this production and decay channel via the Feynman diagram given in Fig. 7. In case of a multi-lepton final state, one ends up with four leptons plus missing energy ($4l + 2\nu_l$), while in case of a multi-hadronic final state one ends up with four jets plus two leptons ($4j + 2l$). In addition, it is also possible to have a mixed final state ($2j + 3l + \nu_l$). If two flavours of the heavy neutrinos are assumed to be degenerate in mass, one gets the same final states for the produced heavy neutrino pair with similar event rates. This will double the number of final state events but will make it difficult to distinguish between final state leptons. Therefore throughout the current study, we consider the non-degenerate heavy neutrino masses also including the interference between every two different flavours. (See Refs. [28, 29, 30, 31, 32, 33] for alternative phenomenological analyses in the case of the standard $B - L$ model.)

In our analysis we have again used SARAH [15] and SPheno [16, 17] to build the model. The matrix element calculation and events generation are derived from MadGraph 5 [18]. Finally we used Pythia [34] to simulate the initial and final state radiation, fragmentation and hadronisation effects. We considered the following benchmark: $M_{Z'} = 1000$ GeV, $M_{\nu_4} = M_{\nu_5} = 287$ GeV, $M_{\nu_6} = M_{\nu_7} = 435$ GeV and $M_{\nu_8} = M_{\nu_9} = 652$ GeV. In addition, the following cuts are assumed: a lower transverse momentum, p_T , cut of 20 GeV (10 GeV) was set on final state jets (electrons) and a pseudo-rapidity, η , cut of 4 (2) was set on jets (electrons) while the separation between two jets (electrons), R_{jj} (R_{ll}), was set to be 0.4 (0.2).

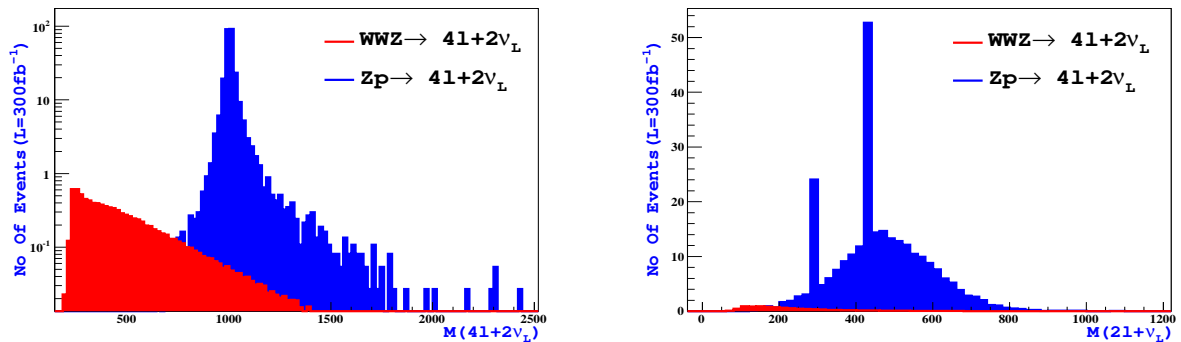


Figure 8: (Left) The invariant mass of the ‘4 leptons plus 2 light neutrinos’ system from Z' decays. (Right) The invariant mass of the ‘2 leptons plus 1 light neutrino’ system from heavy neutrino decays. The expected SM background is included as well (in blue) alongside the signal (red).

Table 4: Number of events after our set of cuts in the case $Z' \rightarrow 4j + 2l$.

Cut	Signal	$ZZjj$	$t\bar{t}$	WW
Initial No. of events	2042	28913	650000	80000
$p_T > 150$ GeV	1088	102	0	0

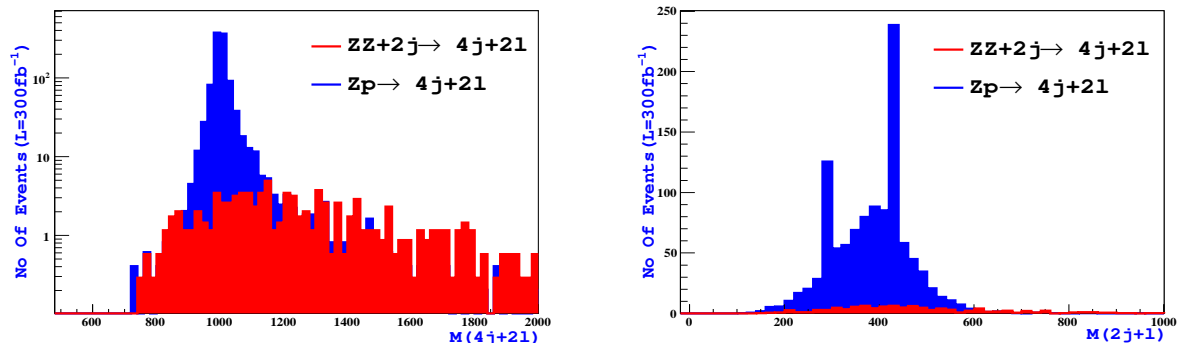


Figure 9: (Left) The invariant mass of the ‘4 jets plus 2 leptons’ system from Z' decays. (Right) The invariant mass of the ‘2 jets plus 1 lepton’ system from heavy neutrino decays. The expected SM background is included as well (in blue) alongside the signal (red).

(i) $4l + 2\nu$ Final State The main advantage of this channel is that it is almost background free. The main SM noise comes from WWZ (three gauge boson) production with $\sigma(WWZ) \sim 200$ fb at 14 TeV [35, 36]. In Fig. 8 we show the generator level invariant mass of the ‘4 leptons plus 2 light neutrinos’ system from the Z' signal versus the WWZ

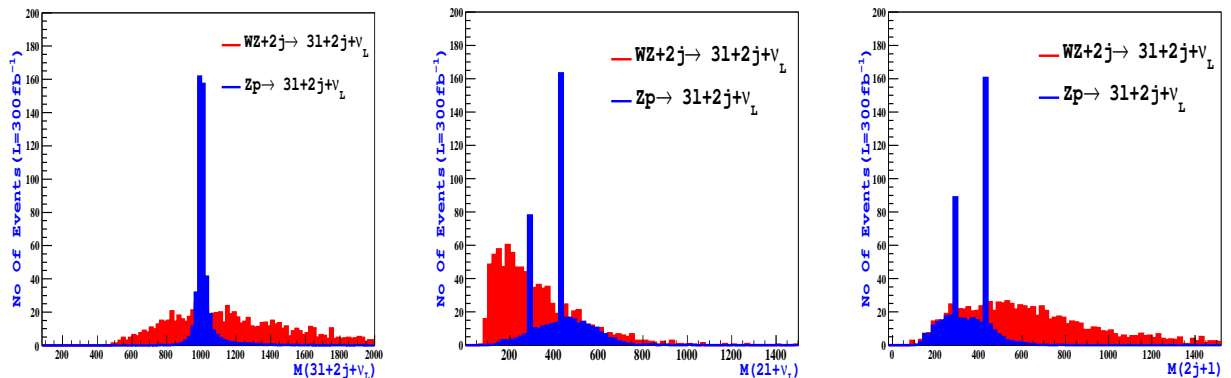


Figure 10: (Left) The invariant mass of $2j + 3l + \nu_l$ from Z' decays. The invariant mass of heavy neutrinos decaying to $2l + \nu$ (Centre) or to $2j + l$ (Right). The expected SM background is included as well (in blue) alongside the signal (red).

background and also the invariant mass of the ‘2 leptons plus light neutrino’ system from the heavy neutrino decay. In the right plot, it is clear that the two heaviest neutrinos (ν_8 and ν_9) decay off-shell when $M_{Z'} = 1000$ GeV. These figures indicate that the decay channel $4l + 2\nu$ yields a quite clean signature and is rather promising for probing both Z' and ν_h using only few simple cuts to extract the signals from the background. The number of events left after the set of cuts mentioned above are 270 for the signal and 10 for the background, for an integrated luminosity of 100 fb^{-1} .

(ii) $4j + 2l$ Final State Here, both W 's decay hadronically and, because of the high BR of $W \rightarrow jj$ ($\sim 60\%$), we expect a larger number of events than in the previous channel. The irreducible SM background is due to $ZZjj$, where one of the Z decays to two leptons while the other decays to quarks ($Z \rightarrow l\bar{l}$, $Z \rightarrow j\bar{j}$). The contribution due to Z +jets can be neglected. In addition, there are two reducible backgrounds coming from $t\bar{t}$ and WW . The number of events left after cuts for signal and backgrounds are listed in Table 4. These are based upon the distributions of Fig. 9, where we present the invariant mass of $4j + 2l$ (left) and also that of the $2j + l$ (right) from both the signal and background, after applying an additional p_T cut of 150 GeV on the two p_T -leading leptons. As in the $4l + 2\nu$ channel, the heaviest two neutrinos (ν_8 and ν_9) are decayed off-shell when $M_{Z'} = 1000$ GeV.

(iii) $2j + 3l + \nu_l$ Final State In the semi-leptonic case where one of the W 's decays hadronically and the other decays to $l\nu_l$ the main background is $WZ + jj$. In the case of $WZ + jj$ associated production, three leptons can be generated from the subsequent lep-

Table 5: Number of events after our set of cuts in the case $Z' \rightarrow 2j + 3l + \nu_l$.

Cut	Signal	$WZjj$
Initial No. of events	769	37975
$p_T > 150$ GeV	475	910

tonic decays of the two gauge bosons. In Fig. 10 we show the invariant mass of $3l + 2j + \nu_l$ (left) for both signal and background. Also the invariant mass of $2l + \nu_l$ (centre) and that of $2j + \nu_l$ (right) is shown therein. Again, an additional $p_T > 150$ GeV cut was set on the two p_T -leading leptons. Table 5 lists the number of events left after cuts for signal and background.

6.2 Search for an Extra BLSSM-IS Higgs Boson

The Higgs decay into $ZZ \rightarrow 4l$ is one of the golden channels, with low background, to search for Higgs boson(s). The search is performed by looking for resonant peaks in the m_{4l} spectrum, *i.e.*, the invariant mass of the $4l$ system. In CMS [37], this decay channel shows two significant peaks at 125 GeV and above 137 GeV. We define by $\sigma(pp \rightarrow h')$ the total h' production cross section, dominated by gluon-gluon fusion. From a previous section, it is then clear that

$$\frac{\sigma(pp \rightarrow h')}{\sigma(pp \rightarrow h)^{\text{SM}}} \simeq \left(\frac{\Gamma_{32}}{\sin \beta} \right)^2, \quad (102)$$

(wherein the label SM identifies the SM Higgs rates computed for a 125 GeV mass), which, for $m_{h'} \approx 137$ GeV, is of order $\mathcal{O}(0.1)$. Also the ratio between BRs can be estimated as

$$\frac{\text{BR}(h' \rightarrow ZZ)}{\text{BR}(h \rightarrow ZZ)^{\text{SM}}} \simeq \left(1 + \frac{\Gamma_{h \rightarrow WW^*}^{\text{SM}}}{\Gamma_{h \rightarrow b\bar{b}}^{\text{SM}}} \right) \frac{F(M_Z/m_{h'})}{F(M_Z/m_h)^{\text{SM}}} \times \left[\left(\frac{\Gamma_{31} \sec \beta}{\Gamma_{32} \sin \beta + \Gamma_{31} \cos \beta} \right)^2 + 2F \left(\frac{M_W}{m_{h'}} \right) \right]^{-1}, \quad (103)$$

where

$$F(x) = \frac{3(1 - 8x^2 + 20x^4)}{(4x^2 - 1)^{1/2}} \arccos \left(\frac{3x^2 - 1}{2x^3} \right) - \frac{1 - x^2}{2x^2} (2 - 13x^2 + 47x^4) - \frac{3}{2} (1 - 6x^2 + 4x^4) \log x^2. \quad (104)$$

Now we analyse the kinematic search for the BLSSM Higgs boson, h' , in the decay channel to $ZZ \rightarrow 4l$. In Fig. 11, we show the invariant mass of the 4-lepton final state from $pp \rightarrow h' \rightarrow ZZ \rightarrow 4l$ at $\sqrt{s} = 8$ TeV, after applying a p_T cut of 5 GeV on the four leptons[12]. The SM model backgrounds from the Z and 125 GeV Higgs boson decays, $pp \rightarrow Z \rightarrow 2l\gamma^* \rightarrow 4l$ and $pp \rightarrow h \rightarrow ZZ \rightarrow 4l$, respectively, are taken into account, as

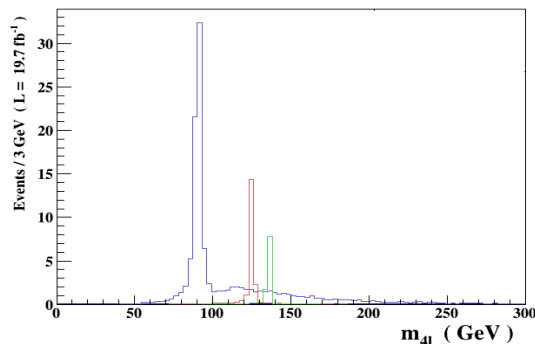


Figure 11: The number of events of the processes $pp \rightarrow Z \rightarrow 2l\gamma^* \rightarrow 4l$ (blue), $pp \rightarrow h \rightarrow ZZ \rightarrow 4l$ (red) and $pp \rightarrow h' \rightarrow ZZ \rightarrow 4l$ (green) versus the invariant mass of the outgoing particles (4-leptons), m_{4l} .

Number of events for 19.7 fb^{-1} at $\sqrt{s} = 8 \text{ TeV}$				
Higgs mass	Observed (CMS)	Expected (BLSSM)	Background	
			$Z \rightarrow 2l\gamma^*$	$h \rightarrow ZZ$
125 GeV	25	18.5	6.6	-
136.5 GeV	29	10.2	9.15	0.8

Table 6: The observed (by CMS) and expected (from the BLSSM) number of events in a mass window around $m_h = 125 \text{ GeV}$ ($121 \text{ GeV} < m_{4l} < 131 \text{ GeV}$) and $m_{h'} = 136.5 \text{ GeV}$ ($131 \text{ GeV} < m_{4l} < 152 \text{ GeV}$) in the $ZZ \rightarrow 4l$ channel compared to the expected (dominant) $pp \rightarrow Z \rightarrow 2l\gamma^* \rightarrow 4l$ and $pp \rightarrow h \rightarrow ZZ \rightarrow 4l$ backgrounds.

demonstrated by the first two peaks in the plot (with the same p_T requirement). It is clear that the third peak at $m_{4l} \sim 137 \text{ GeV}$, produced by the decay of the BLSSM Higgs boson h' into $ZZ \rightarrow 4l$, can reasonably well account for the events observed by CMS [37] with the 8 TeV data. This is shown in Table 6, where the mass interval in m_{4l} that we have investigated to extract the h' signal is wide enough to capture the prominent 145 GeV anomaly seen in CMS.

Now we turn to the di-photon channel, which provides the greatest sensitivity for Higgs boson discovery in the intermediate mass range (*i.e.*, for Higgs masses below $2M_W$)⁵. Like the SM-like Higgs, the h' decays into two photons through a triangle-loop diagram dominated by (primarily) W and (in part) top quark exchanges. As shown in a previous

⁵The effects of light SUSY particles leading to a possible enhancement of the di-photon signal strength of the SM-like Higgs boson were studied in [38].

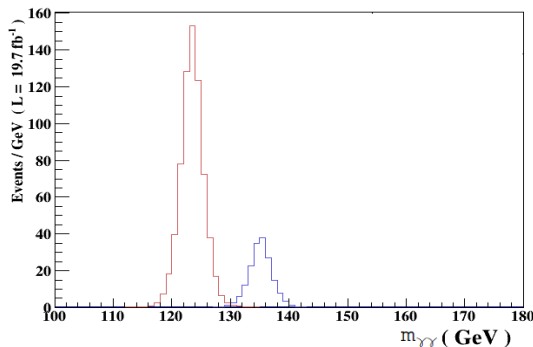


Figure 12: The number of events of the processes $pp \rightarrow h \rightarrow \gamma\gamma$ (red), $pp \rightarrow h' \rightarrow \gamma\gamma$ (blue) versus the invariant mass of the outgoing particles (di-photons), $m_{\gamma\gamma}$.

Number of events for 19.7 fb^{-1} at $\sqrt{s} = 8 \text{ TeV}$		
Higgs mass	Observed (CMS)	Expected (BLSSM)
125 GeV	610	666
136.5 GeV	170	177

Table 7: The observed (by CMS) and expected (from the BLSSM) number of events (after subtracting background) in a mass window around $m_h = 125 \text{ GeV}$ ($120 \text{ GeV} < m_{\gamma\gamma} < 130 \text{ GeV}$) and $m_{h'} = 136.5 \text{ GeV}$ ($131 \text{ GeV} < m_{\gamma\gamma} < 141 \text{ GeV}$) in the $\gamma\gamma$ channel.

section, the couplings of the h' with top quarks and W gauge bosons are proportional to some combinations of Γ_{31} and Γ_{32} , which may then lead to some suppression in the partial width $\Gamma(h' \rightarrow \gamma\gamma)$. In the SM, $\text{BR}(h \rightarrow \gamma\gamma) \simeq 2 \times 10^{-3}$. Similarly, in the BLSSM, we found that, for $m_{h'} = 136.5 \text{ GeV}$, the BR of h' in photons amounts to 2.15×10^{-3} .

The distribution of the di-photon invariant mass is presented in Fig. 12 for a centre-of-mass energy $\sqrt{s} = 8 \text{ TeV}$ [12]. Again, here, the observed $h \rightarrow \gamma\gamma$ SM-like signal around 125 GeV is taken as background while the $Z \rightarrow \gamma\gamma$ background can now be ignored [39]. As expected, the sensitivity to the h' Higgs boson is severely reduced with respect to the presence of the already observed Higgs boson, yet a peak is clearly seen at 136.5 GeV and is very compatible with the excess seen by CMS [14]. This is shown in Table 7. It is worth mentioning that here we consider both the gluon-gluon fusion and vector-boson fusion modes for both h and h' production.

Before closing this section, we should also mention that the $h' \rightarrow \gamma\gamma$ enhancement found in the BLSSM may be mirrored in the γZ decay channel [13] for which, at present, there exists some constraints, albeit not as severe as in the $\gamma\gamma$ case. We can anticipate

(see [13]) that the BLSSM regions of parameter space studied here are consistent with all available data.

7 Conclusions

In summary, in this mini-review, we have introduced the reader to the minimal SUSY version of the well established $B - L$ model with an IS mechanism, that we have termed as BLSSM. This scenario nicely combines the theoretically appealing features of SUSY with key experimental evidence of Beyond the SM (BSM) physics in the form of neutrino masses.

Initially, we have proceeded with the construction of the BLSSM Lagrangian, followed by an illustration of how dynamical EWSB naturally occurs via RGE evolution starting from an mSUGRA inspired model configuration at high scales. Then, we have described the emerging particle spectrum, by singling out the dynamics in the three specifically BLSSM sectors: *i.e.*, the Z' , Higgs and (s)neutrino parts. In three separate subsections we have in fact derived the relevant masses and couplings.

As EWSB and $B - L$ breaking both occur close to the SUSY mass scale of order 1 TeV, the BLSSM also bears interesting phenomenological manifestations at the LHC in the three aforementioned sectors. Therefore, we have studied next the hallmark signals of this scenario in turn. Firstly, we described Z' production and decay into a variety of leptonic and hadronic signatures proceeding via heavy neutrinos⁶, all leading to detectable signals at run 2 of the CERN machine. Secondly, we highlighted the striking feature of the BLSSM in the Higgs sector, in the form of a possible additional light Higgs resonance yielding sizable $\gamma\gamma$ and ZZ decays which may even explain some anomalies around a mass of 140 GeV present already in the CMS data of run 1 of the LHC.

In short, the BLSSM represents a viable realisation of SUSY, compliant with all current data and giving distinctive signatures at the LHC which will enable one to disentangle it from alternative BSM scenarios.

Acknowledgements

The work of SK is partially supported by the ICTP grant AC-80. SM is supported in part through the NExT Institute. The work of SK and SM is also funded through the grant H2020-MSCA-RISE-2014 no. 645722 (NonMinimalHiggs).

⁶The case of sneutrino mediated channels is now being tackled in Ref. [40].

References

- [1] S. Khalil, J. Phys. G **35**, 055001 (2008).
- [2] S. Khalil, Phys. Rev. D **82**, 077702 (2010).
- [3] R. N. Mohapatra and R. E. Marshak, Phys. Rev. Lett. **44**, 1316 (1980) [Erratum-ibid. **44**, 1643 (1980)];
C. Wetterich, Nucl. Phys. B **187**, 343 (1981);
W. Buchmuller, C. Greub and P. Minkowski, Phys. Lett. B **267**, 395 (1991);
W. Buchmuller and T. Yanagida, Phys. Lett. B **302**, 240 (1993).
- [4] S. Khalil and A. Masiero, Phys. Lett. B **665**, 374 (2008).
- [5] A. El-Zant, S. Khalil and A. Sil, Phys. Rev. D **91**, 035030 (2015).
- [6] L. Basso, B. O’Leary, W. Porod and F. Staub, JHEP **1209**, 054 (2012).
- [7] S. Khalil, O. Seto, JCAP **0810**, 024 (2008)
- [8] S. Khalil and S. Moretti, J. Mod. Phys. **4**, 7 (2013).
- [9] S. Khalil and S. Moretti, Front. Phys. **1**, 10 (2013).
- [10] W. Abdallah, A. Awad, S. Khalil and H. Okada, Eur. Phys. J. C **72**, 2108 (2012).
- [11] B. O’Leary, W. Porod and F. Staub, JHEP **1205**, 042 (2012).
- [12] W. Abdallah, S. Khalil and S. Moretti, Phys. Rev. D **91**, 014001 (2015).
- [13] A. Hammad, S. Khalil and S. Moretti, arXiv:1503.05408 [hep-ph].
- [14] CMS Collaboration, CMS-PAS-HIG-13-016.
- [15] F. Staub, arXiv:0806.0538 [hep-ph].
- [16] W. Porod, Comput. Phys. Commun. **153**, 275 (2003).
- [17] W. Porod and F. Staub, Comput. Phys. Commun. **183**, 2458 (2012).
- [18] J. Alwall et al., JHEP **1407**, 079 (2014).
- [19] E. Conte, B. Fuks and G. Serret, Comput. Phys. Commun. **184**, 222 (2013).
- [20] A. Elsayed, S. Khalil, S. Moretti and A. Moursy, Phys. Rev. D **87**, 053010 (2013).

- [21] A. Elsayed, S. Khalil and S. Moretti, Phys. Lett. B **715**, 208 (2012).
- [22] S. Khalil, H. Okada and T. Toma, JHEP **1107**, 026 (2011).
- [23] J. M. Frere, D. R. T. Jones and S. Raby, Nucl. Phys. B **222**, 11 (1983).
- [24] A. A. Abdelalim, A. Hammad and S. Khalil, Phys. Rev. D **90**, 115015 (2014).
- [25] G. Arcadi, Y. Mambrini, M. H. G. Tytgat and B. Zaldivar, JHEP **1403**, 134 (2014).
- [26] ATLAS Collaboration, ATLAS-CONF-2013-017.
- [27] CMS Collaboration, arXiv:1212.6175v2.
- [28] L. Basso, A. Belyaev, S. Moretti and C. H. Shepherd-Themistocleous, Phys. Rev. D **80**, 055030 (2009).
- [29] L. Basso, A. Belyaev, S. Moretti and G. M. Pruna, JHEP **0910**, 006 (2009).
- [30] L. Basso, A. Belyaev, S. Moretti, G. M. Pruna and C. H. Shepherd-Themistocleous, PoS EPS **HEP2009**, 242 (2009).
- [31] M. Abbas and S. Khalil, JHEP **0804**, 056 (2008).
- [32] W. Emam and S. Khalil, Eur. Phys. J. C **52**, 625 (2007).
- [33] K. Huitu, S. Khalil, H. Okada and S. K. Rai, Phys. Rev. Lett. **101**, 181802 (2008).
- [34] T. Sjostrand, S. Mrenna and P. Skands, Comput. Phys. Commun. **178**, 852 (2008).
- [35] V. D. Barger and T. Han, Phys. Lett. B **212**, 117 (1988).
- [36] V. Hankele and D. Zeppenfeld, Phys. Lett. B **661**, 103 (2008).
- [37] CMS Collaboration, Phys. Rev. D **89**, 092007 (2014).
- [38] A. Belyaev, S. Khalil, S. Moretti and M. C. Thomas, JHEP **1405**, 076 (2014);
M. Hemed, S. Khalil and S. Moretti, Phys. Rev. D **89**, 011701 (2014);
J. A. Casas, J. M. Moreno, K. Rolbiecki and B. Zaldivar, JHEP **1309**, 099 (2013);
A. Djouadi, V. Driesen, W. Hollik and J. I. Illana, Eur. Phys. J. C **1**, 149 (1998);
A. Arbey, M. Battaglia, A. Djouadi, F. Mahmoudi and J. Quevillon, Phys. Lett. B **708**, 162 (2012);
S. Heinemeyer, O. Stal and G. Weiglein, Phys. Lett. B **710**, 201 (2012);

L. J. Hall, D. Pinner and J. T. Ruderman, JHEP **1204**, 131 (2012)

M. Carena, S. Gori, N. R. Shah and C. E. M. Wagner, JHEP **1203**, 014 (2012)

K. Schmidt-Hoberg and F. Staub, JHEP **1210**, 195 (2012);

L. Basso and F. Staub, Phys. Rev. D **87**, 015011 (2013).

[39] S. Moretti, Phys. Rev. D **91**, 014012 (2015).

[40] W. Abdallah, J. Fiaschi, S. Khalil and S. Moretti, in progress.